

## Article

# Biochar Grafted on CMC-Terpolymer by Green Microwave Route for Sustainable Agriculture

Shimaa M. Elsaeed <sup>1,\*</sup>, E. G. Zaki <sup>1</sup>, Tarek M. Ibrahim <sup>2</sup>, Nasser Ibrahim Talha <sup>2</sup>, Hosam A. Saad <sup>3</sup>, Adil A. Gobouri <sup>3</sup>, Amr Elkelish <sup>4</sup> and Salah Mohamed el-kousy <sup>5</sup>

<sup>1</sup> Egyptian Petroleum Research Institute, P.O. Box 11727, Cairo, Egypt; chemparadise17@yahoo.com

<sup>2</sup> Soil, Water and Environment Research Institute, ARC, P.O. Box 12411, Giza, Egypt; Tarekibrahim7979@gmail.com (T.M.I.); nassertalha89@yahoo.com (N.I.T.)

<sup>3</sup> Department of Chemistry, College of Science, Taif University, P.O. Box 11099, Taif 21944, Saudi Arabia; h.saad@tu.edu.sa (H.A.S.); a.gobouri@tu.edu.sa (A.A.G.)

<sup>4</sup> Botany Department, Faculty of Science, Suez Canal University Ismailia, Ismailia 41522, Egypt; Amr.elkelish@science.suez.edu.eg

<sup>5</sup> Chemistry Department, Faculty of Science, Menofiya University, P.O. Box 32513, Shebine El-kom, Egypt; elkousy43@yahoo.com

\* Correspondence: shy\_saeed@yahoo.com

**Abstract:** The deficiency of water sources and the environmental disposal of large amounts of biomass waste (orange peels) produces economic and environmental problems, though its conversion into biochar by a pyrolysis procedure might be used to improve soil productivity. In the current study, we investigated the performance of superabsorbent biochar composite grafted on CMC as a low-cost, alternative, and biodegradable terpolymer composite (IPNCB) for soil water retention capacity. The IPNCB composite was synthesized by both microwave and conventional routes. The optimal reaction parameters proved that the microwave route has a high grafting percentage (%G) and short reaction time compared to the conventional route. The superabsorbent composite was characterized using different methods: FTIR, TGA, and SEM. The results show that the equilibrium water swelling (EW) of the IPNCB composite was improved at a 2% biochar concentration. The incorporation of biochar (BC) into the polymer network improved the water holding capacity (WHC) to 57.6% and water retention (WR) to 9.1% after 30 days. The degradation test indicates the IPNCB composite has a good degradability rate. Mixing soil with the prepared IPNCB composite can improve plant growth and reduce water consumption through the irrigation of arid lands. The IPNCB composite is a candidate in sustainable agriculture applications.

**Keywords:** biochar; superabsorbent; swelling ratio and water retention; water holding capacity



**Citation:** Elsaeed, S.M.; Zaki, E.G.; Ibrahim, T.M.; Ibrahim Talha, N.; Saad, H.A.; Gobouri, A.A.; Elkelish, A.; Mohamed el-kousy, S. Biochar Grafted on CMC-Terpolymer by Green Microwave Route for Sustainable Agriculture. *Agriculture* **2021**, *11*, 350. <https://doi.org/10.3390/agriculture11040350>

Academic Editors: Zakaria Solaiman and Hossain Md Anawar

Received: 26 February 2021

Accepted: 11 April 2021

Published: 14 April 2021

**Publisher's Note:** MDPI stays neutral with regard to jurisdictional claims in published maps and institutional affiliations.



**Copyright:** © 2021 by the authors. Licensee MDPI, Basel, Switzerland. This article is an open access article distributed under the terms and conditions of the Creative Commons Attribution (CC BY) license (<https://creativecommons.org/licenses/by/4.0/>).

## 1. Introduction

Water scarcity is a serious problem in various regions around the world, especially due to climate change. Water is the main factor for crop production and cultured zones [1]. The development of agriculture depends on solving these problems, and a potential method is using materials with high water absorption called superabsorbent hydrogels.

Superabsorbent hydrogels (SAPs), which can be used as water management resources for agricultural development, have recently attracted attention for their increased water holding capacity, decreased irrigation rate, and ability to enhance growth of plants and save water consumption [2]. These materials consist of three-dimensional networks and are mainly divided into chemical and physical crosslinking according to the material used. Chemical crosslinking can form hydrogels rapidly under mild condition with addition of crosslinker. Physically crosslinked hydrogels have electrostatic interaction, hydrogen bonds, hydrophobic interaction, and van der Waals force between the polymers without the addition of ionic crosslinking agents.

Superabsorbent hydrogels are broadly applied in several fields such as agriculture [3,4] wastewater treatment [5–7], biosensors, drug release [8], self-healing [9], tissue engineering [10], adsorbents for organic [11], inorganic pollutants [12,13], and enhanced oil recovery [14,15]. Usually, superabsorbent hydrogels based on synthetic polymers, compared with those based on natural polymers such as chitosan [16], cellulose [17], starch [18], and their substitutes, are of great interest due to their eco-friendly properties and low cost, non-toxicity, biodegradability, and highly hydrophilic network [19].

The most abundant biopolymer in Egypt is carboxy methyl cellulose, CMC, a water soluble ionic derivative of cellulose. It is the most significant ionic cellulose ether with worldwide production. The main target is to use CMC as a core for superabsorbent hydrogel for water retention, soil conditioning, and fertilizer delivery to decrease the huge loss in agriculture [17,20–22]. Superabsorbent hydrogels are mainly built on non-biodegradable resources, for example polyacrylates. Many researchers made efforts to develop eco-friendly and low-cost superabsorbent polymers to overcome poor biodegradability and high costs of SAP based on acrylates by using biomass waste and clays embedded in the polymer matrix [21,23].

Farmers in many countries especially in Egypt have become interested in applying organic recycling materials for use in the agriculture sector. Biomass wastes available in Egypt are an abundant source of biochar. Biochar is a carbon material that is produced from the pyrolysis of biomass waste. Biochar may be applied in combined plans to improve soil quality and raise productivity. Biochar has a unique adsorption property due to its high surface area [24]. The polymer/biochar composite is usually applied because of its low cost and high adsorption capacity for water pollution and in soil fertilizer. The ability of superabsorbent hydrogel/biochar composite to uptake aqueous solutions is due to the function groups connected to the composite backbone [25]. Therefore, conversion of biomass waste to biochar reduces the negative effect of organic wastes on the environment and helps to alleviate contamination, landfill, and economic impact.

The incorporation of biochar into polysaccharides not only decreases costs but also improves the properties (e.g., gel strength, swelling ability, mechanical and thermal stability) of hydrogels and accelerates the generation of new materials for special application.

In this study, through pyrolysis of biomass waste (orange peel waste to obtained biochar), a unique green superabsorbent hydrogel-based biochar was prepared by grafting of biochar based on copolymerization of AA, Am, and AMPS monomers along the chains of CMC using the microwave and conventional techniques. The microwave route enhanced swelling ratio, water retention, and water holding capacity, making the process suitable for sustainable agriculture. The microwave technique is considered a green route alternate to the traditional route, which is based on the thermal method and has a lengthy and energy-consuming process. Microwave synthesis is a simple, high-productivity, low-energy, and low-cost process that leads to less contamination and fewer byproducts. The swelling properties of the prepared composite CMC-g-(Am-AMPS-AA)/Biochar (IPNCB) in different solutions (water, 0.9% NaCl) and different buffers were systematically studied. The composite synthesis of the interpenetrating superabsorbent composite IPNCB was characterized through infrared spectroscopy, scanning electron microscopy, and thermal analysis. Water retention and degradation rate of prepared superabsorbent composite was evaluated.

Our objective was the synthesis of the green superabsorbent composite IPNCB with unique properties and high swelling and minimal reaction time via the green microwave route. WHC and WR performance show that this process can be considered suitable for sustainable agriculture applications.

## 2. Materials and Methods

### 2.1. Materials

Carboxy methyl cellulose (CMC) and orange peel biochar were obtained locally from Shibin El Kom, Egypt. Sandy soil was acquired from El-Hamoul, Egypt, while

acrylic acid (AA), acrylamide (AM), acrylamide-co-2-acrylamido-2-methylpropane sulfonic acid (AMPS), potassium persulfate (KPS), N, N' methylene bisacrylamide (MBA), NaOH, ethanol, and methanol were purchased from Sigma-Aldrich. Table 1 clarifies the properties of biochar.

**Table 1.** Elemental composition (%) of biochar (BC).

Sample	C	H	N	O	S
BC	67.43	4.91	1.12	25.21	0.33

## 2.2. Biochar Production

Orange peel waste was collected, dried at 70 °C, and pyrolyzed in an oven under N<sub>2</sub> at 350 °C for 3 h [26]. The produced biochar was ground, washed with 0.1 M HCl for 5 h, washed with distilled water to remove any impurities, and then dried in an oven at 70 °C for 24 h. Table 1 shows the estimated elemental composition of biochar.

## 2.3. Sandy Soil

The sandy soil sample was collected from the El-Hamoul area (31-07' N Latitude, 30-57' E Longitude, with an elevation of about 6 m above mean sea level), Kafr El-Sheikh Governorate, Egypt. Physical and chemical properties of the studied soil samples, which were determined using the appropriate methods as described by Kim et al. [27], are presented in Table 2.

**Table 2.** Chemical and physical characteristics of the studied soil.

Parameter	Value	Parameter	Value
<b>Soil Chemical Properties</b>			
EC (dS/m)	0.52	Cl <sup>-</sup> (meq/L)	1.50
pH	7.88	SO <sub>4</sub> <sup>-2</sup> (meq/L)	2.35
Na <sup>+</sup> (cmol+ kg <sup>-1</sup> )	1.25	CaCO <sub>3</sub> (%)	1.08
Ca <sup>++</sup> (cmol+ kg <sup>-1</sup> )	2.75	SAR	6.04
Mg <sup>+</sup> (cmol+ kg <sup>-1</sup> )	0.55	OM (%)	0.40
K <sup>+</sup> (cmol+ kg <sup>-1</sup> )	0.38	Available N (mg/kg)	28.9
CO <sub>3</sub> = (cmol+ kg <sup>-1</sup> )	0.0	Available P (mg/kg)	6.85
HCO <sub>3</sub> <sup>-</sup> (cmol+ kg <sup>-1</sup> )	5.5	Available K (mg/kg)	65.5
<b>Soil Physical Properties</b>			
Bd (Mg/m <sup>3</sup> )	1.58	FC (%)	18.2
Ks (m/day)	2.70	PWP (%)	8.6
SP (%)	34.0	AWC (%)	9.6
<b>Particle Size Distribution (%)</b>			
Sand	84.8	Clay	9.6
Silt	5.6	Texture	Sandy

EC: Soil salinity as electrical conductivity; Bd: Soil bulk density; Ks: Saturated hydraulic conductivity; FC: Soil field capacity; PWP: Soil permanent wilting point; AWC: Soil available water content.

## 2.4. Preparation of CMC-g-(TerPols)/BC by Conventional Method

The synthesis of CMC-g-TerPols superabsorbent hydrogel was achieved using a free radical polymerization technique. CMC is soluble in a specific quantity of d-water. At that point, two different weight ratios (1% and 2%) of biochar (BC) were added and sonicated for 20 min to form homogeneous dispersed solution. Added NaOH with a concentration 4 mol/L solution was utilized to neutralize the solution, and AA, Am, and AMPS were added consistently. When the temperature reached 70 °C, the amount of KPS in d-water was added to the mixture. After mixing for 15 min and decreasing the temperature to 40 °C, MBA in d-water was added to all the mixture with a purge of N<sub>2</sub>. The water bath

was kept at 70 °C to complete the polymerization reaction for 3 h [28] to get CMC-g-(TerPols)/biochar (IPNBC). This gel was cut into little pieces and washed by a suitable ratio of distilled water and ethanol to remove the unreacted monomers and other chemicals. The IPNBC was formed and dried overnight in an oven at 60 °C. The graft yield or percentage grafting (G) was calculated using Equation (1):

$$G = [(W1 - WO)/WO] \times 100 \quad (1)$$

where WO and W1 denote the weight of CMC and graft copolymer, respectively. The composition of CMC superabsorbent hydrogels is illustrated in Table 3.

**Table 3.** Optimized chemical composition of CMC-g-(TerPols)/BC superabsorbent composite.

Samples	CMC (g)	Ac (mL)	Am (g)	AMPS (g)	BC (%)	KPS (g)	MBA (g)
IPNCB	5	3	3	3	1, 2	0.7	0.5

### 2.5. Preparation of CMC-g-(TerPols)/BC by Microwave Method

CMC is soluble in a specific quantity of d-water. At that point, two different weight ratios (1% and 2%) of biochar (BC) were added and sonicated for 20 min to form homogeneous dispersed solution. NaOH with a concentration 4 mol/L solution was utilized to neutralize the solution, and AA, Am, and AMPS were added consistently. Then KPS and MBA in d-water were added to the mixture with a purge of N<sub>2</sub>. The solution was kept in the microwave reactor at 800 W, and the temperature was set to 70 °C for diverse timing. After the completion of reaction time the gel obtained was cut into little pieces and washed using a suitable ratio of distilled water and ethanol to remove the unreacted monomers and other chemicals. The IPNBC was formed and dried overnight in an oven at 60 °C. The graft yield or (%) grafting was calculated using Equation (1).

### 2.6. Swelling Behavior in Different Media and Equilibrium Water Absorbance of (CMC-TerPols)/BC Superabsorbent Composite

The equilibrium water absorbance and swelling of synthesized hydrogel were measured by immersing 0.5 g of dried IPNBC composite in d-water (200 mL) to reach swelling equilibrium state (Q<sub>eq</sub>) [29]. The swollen gel was filtered from the solution and dried. The swollen gel was then weighed, and the Equilibrium water absorbance was calculated with Equation (2):

$$Q_{eq} = [(W_s - W_d)/W_d] \times 100 \quad (2)$$

where Q<sub>eq</sub> is the equilibrium water absorbance (g/g) (EW) at time t (min), W<sub>s</sub> is swollen hydrogel (g), and W<sub>d</sub> is dried hydrogel (g).

Swelling behavior of the CMC-g-(TerPols) superabsorbent in saline water (s-water) 0.9 wt% NaCl solution and several buffer mediums was measured as follows: 0.5 g of the superabsorbent was placed in 500 mL beakers into which 100 mL of saline or buffer solution was then poured. The swollen gels were then filtered, and the swelling behavior of IPNBC was calculated according to the above Equation (2).

### 2.7. Water Retention (WR) and Water Holding Capacity (WHC) of Soil with IPNCB Composite

The WHC% and WR% of soil with IPNCB are the main properties used to investigate the capacity of IPNBC composite to hold and retain the water inside its network matrix [30]. They were measured by taking 100 g of dry soil only (A), 100 g of dry soil mixed with 1.0 g of IPNCB (B), and 100 g of dry soil mixed with 2.0 g of IPNCB (C). Each sample was placed in a sealed tube with 200-mesh nylon fabric and weighed (WO). The (A), (B), and (C) samples were slowly soaked with d-water until saturation, and then the samples were weighed again (W1). The WHC % of the soil was calculated using Equation (3).

$$WHC \% = [(W1 - WO)/WO] \times 100 \quad (3)$$

The WR % of the soil with the IPNCB composite was calculated by Equation (4), and the A, B, C samples were kept under the same conditions and weighed every 3 days ( $W_i$ ) for 30 days.

$$WR \% = [(W_i - W_0)/(W_1 - W_0)] \times 100 \quad (4)$$

### 2.8. Degradation Rate (DR) of IPNCB Composite in Soil

The degradation rate of the IPNCB composite was determined by measuring the weight loss of the IPNCB composite with the incubation time in soil. The IPNCB composite (0.1 g) was stored in a nylon bag and then placed 5 cm under the surface of the soil and incubated for up to 30 days. The bags of IPNCB were then picked out at various times (5, 10, 15, 20, 25, and 30 days), washed and dried until constant weight, and then the IPNCB composite was weighed to calculate the weight loss with Equation (5).

$$DR \% = [(W_0 - W_i)/W_0] \times 100 \quad (5)$$

where  $W_0$  and  $W_i$  are the weights of the IPNCB before and after degradation (g), respectively.

### 2.9. Characterization of IPNBC Superabsorbent Composite

The chemical structures were confirmed using Fourier transform infrared spectroscopy (ATI Matson Genesis Series FTIR™). The thermal properties of the prepared hydrogels were measured by using samples that were thermogravimetrically analyzed using a TGA 55 (Meslo, Sante Fe Springs, CA, USA). Film samples were placed in a pan of platinum and heated in the range of 300 to 800 °C under N<sub>2</sub> atmosphere at a heating rate of 10 °C per minute, and weight loss was plotted versus temperature.

The morphology of the gel (freeze-dried for 24 h) was observed by using scanning electron microscopy (SEM). The surface images of hydrogels were recorded using a Quanta FEG 250 scanning electron microscope (FEI Company, Hillsboro, OR, USA) available from EDRC, DRC, and Cairo. Samples were mounted onto SEM stubs. Applied SEM conditions were a 10.1 mm working distance, with an in-lens detector with an excitation voltage of 20 kV.

## 3. Results and Discussion

### 3.1. Synthesis of CMC-g-(TerPolys)/BC Composite and Spectral Analysis

Figure 1 verifies the predicted mechanism of graft polymerization. The crosslinking procedure of AA, AMPS, and Am onto CMC chains was achieved both by conventional and microwave methods. This was carried out by using APS as a radical initiator and MBA as a crosslinking agent. APS was decomposed by heating to give sulfate radicals, which pull hydrogen atoms from the -OH groups of the CMC matrix to create macroradicals. AA, Am, and AMPS monomers can be grafted onto these active macroradicals and MBA in this stage to crosslink monomers with radicals on the CMC matrix to form a three-dimensional interpenetrating network-IPN structure. Through the formation of a 3D IPN network, BC was dispersed and bounded in a superabsorbent interpenetrating network.

The grafting and BC incorporation into the superabsorbent IPN were confirmed by comparing the FTIR spectra of CMC, BC, and IPNBC composite.

The FTIR spectra Figure 2a–c of the CMC-g-(TerPolys)/BC superabsorbent composite were compared. As shown in Figure 2a, of the biochar spectrum, the absorption bands at 805 and 915 cm<sup>-1</sup> are related to the aromatic C-H out-of-plane bending vibration, the band at 1701 cm<sup>-1</sup> is assigned to the C=O group, and the band at 1066 cm<sup>-1</sup> is assigned to stretching C-N and C-O.

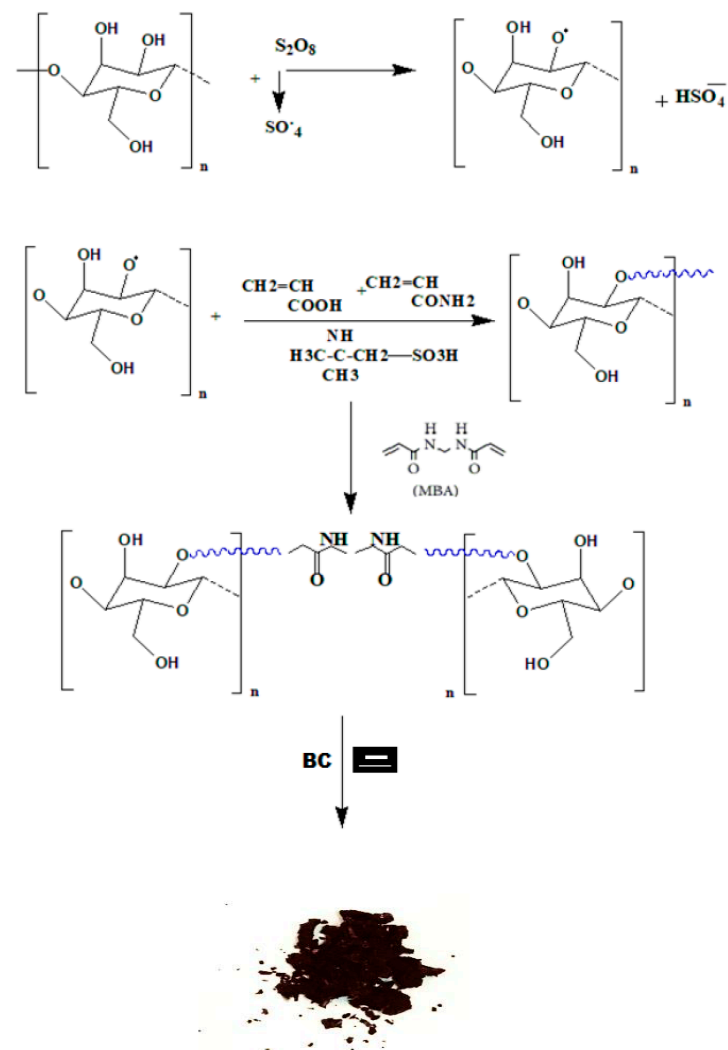


Figure 1. Scheme of synthesized CMC-g-(TerPolys)/BC composite.

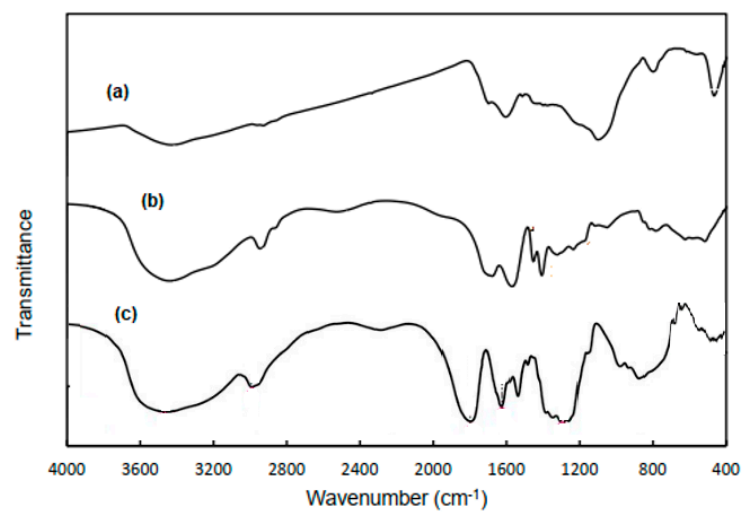


Figure 2. FTIR spectra of (a) biochar, (b) CMC-g-(TerPolys)/biochar composite, (c) CMC.

The shifting of the peak at  $3437.7\text{ cm}^{-1}$  is attributed to -OH stretching of CMC, and the band of CMC at  $1000\text{--}1166\text{ cm}^{-1}$  is reduced due to the contribution of -OH of CMC in reaction (Figure 2b,c).

The characteristic band at  $1548$ ,  $1670$ , and  $1040\text{ cm}^{-1}$  is due to carboxylate anions, carboxamide, and sulfonate groups, respectively. The introduction of  $\text{COO}^-$ ,  $\text{-CONH}$ , and  $\text{-SO}_3^-$  was therefore helpful for the water absorbency of the composite because of their hydrophilic nature. Moreover, the presence of the hydrophilic functional groups and BC in the polymeric matrix were also beneficial to the water absorbency [31].

### 3.2. Optimization Parameters

#### 3.2.1. Optimization Time

Improving the optimization of the time of the reaction is crucial to improving graft yield (G%). The optimized time for the conventional method was 70 min, while in microwave synthesis, it was nearly 12 min. The graft yield (G%) of the two techniques is 7.8, which was reached at the termination stage. Any increase in the reaction time decreased the G% due to the reduction of active groups and predictable homopolymer creation [32]. The microwave method is therefore faster and more promising when compared to the conventional method, and the improved G% was achieved with minimal reaction time (12 min). The swelling behavior was also improved.

Our aim was to prepare a green superabsorbent composite with a 12 min reaction time and high swelling. WHC and WR performance was considered suitable for other studies. We studied the different optimization parameters (initiator, monomer, and crosslinker concentration) that affect graft yield using the microwave technique.

#### 3.2.2. Optimum Initiator and Monomer Ratio

Figure 3 shows the optimization ratio of initiator required to reach the high %G of IPNBC composite using the microwave technique. The maximum and optimal ratio of initiator was 0.7 g. Any excess of initiator concentration is damaged graft yield (G%); this may be due to the creation of many free radicals and homopolymers, which leads to smaller chains of the polymer matrix [33]. The findings outlined in Figure 4 show that 3 g of monomer reached the optimum %G, increasing grafting values continuously, and then decreased along with the monomer concentration mentioned above, so the %G decreased. This may be because any increase of monomer leads to the creation of homopolymers and a reduction of active sites on the CMC matrix through polymerization, which decreases graft yield (%G) [34].

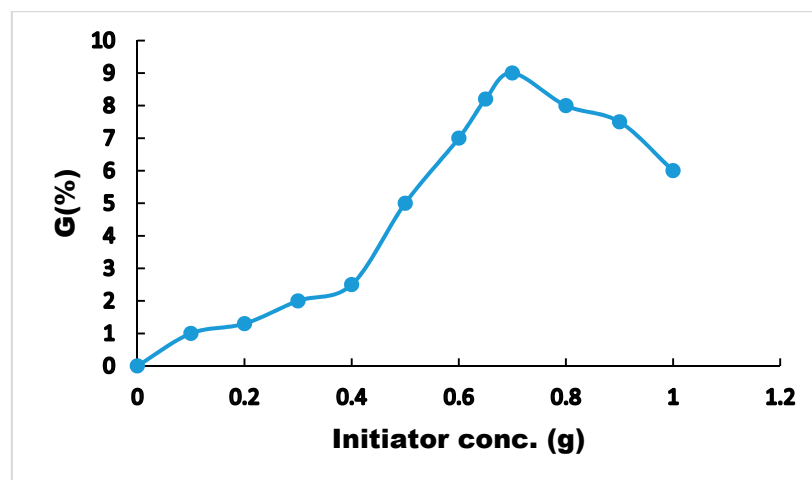


**Figure 3.** Optimum initiator concentration for microwave synthesis of the Interpenetrating Network Biohar Composite (IPNBC).

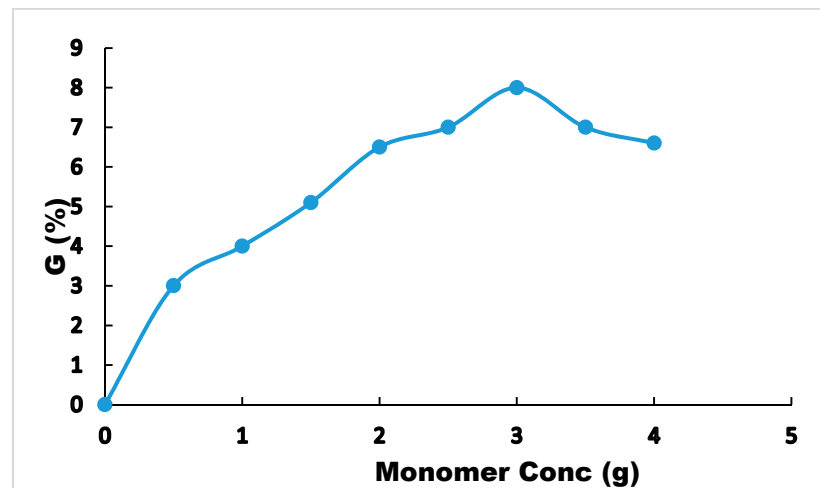


**Figure 4.** Optimum monomer concentration for microwave synthesis of the Interpenetrating Network Biochar Composite (IPNCB).

### 3.2.3. Optimum Crosslinker Ratio

The effect of crosslinker ratio on the swelling performance was studied by taking 0.3 g of the IPNCB composite produced with different ratios of crosslinker (0.02–0.5 g), which was added to small beakers with distilled water. The samples were kept until swelling of the IPNCB composite, and the EW was calculated as given in Equation (2). From Table 4 it can be seen that the maximum swelling was recorded at 0.5 g of crosslinker ratio, then decreased with further addition. This may be attributed to Flory's theory; the swelling behavior of any polymeric matrix is related to the crosslinked density [35]. In radical polymerization, a high crosslinker ratio will provide many crosslinking sites and raise the crosslinked density. Therefore, the network space for holding water was lessened, i.e., the water absorbance capacity decreased [36].

**Table 4.** Optimization crosslinker concentration in CMC-g(TerPolys)/BC superabsorbent composite.

Crosslinker (MBA) Concentration (g)	Equilibrium Swelling (EW) of IPNCB
0.02	1075
0.04	1200
0.06	1520
0.1	1730
0.5	1900

### 3.3. Morphological Analysis SEM

Two of the most significant properties of superabsorbent hydrogels are porosity and pore size. SEM morphologies of the CMC-g-(TerPolys)/BC, and biochar (BC) are shown in Figure 5a,b, respectively. The BC in Figure 5a shows pores and high surface area that lead to a high number of adsorption sites over a short time, allowing much more water to be held in pores during irrigation [37]. Figure 5b shows that in IPNCB, the pore size is smaller and the composite has a rough surface, which was due to the formation of crosslinked network, which was enhanced due to the diffusion of water into the IPN composite and increased swelling rate. These SEM results established that the BC was finely spread in the composite to form a homogeneous composition.

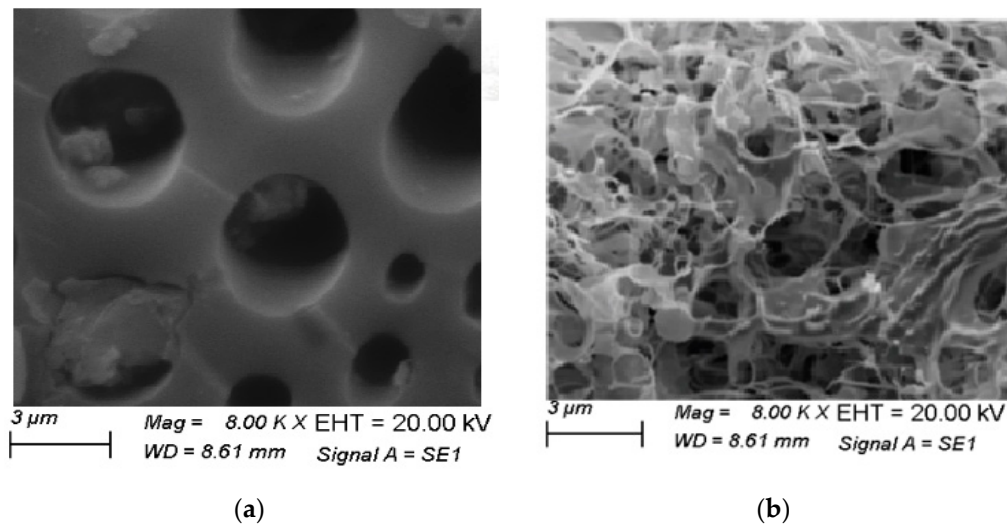


Figure 5. SEM morphology of (a) BC, (b) IPNCB.

#### 3.4. Thermogravimetric Analysis (TGA)

The effect of the grafting and crosslinking of monomer chains onto CMC and interpenetration of biochar within the CMC matrix on the thermal stability was studied. The thermal stability of the CMC, BC, and IPNCB were evaluated by comparing the weight loss (%) in the temperature range of 100 to 600 °C as shown in Figure 6. A three-stage decomposition mechanism was found, and maximum weight loss was observed after the first stage decomposition of crosslinked samples, indicating the chemical modification of CMC. In all cases initial decomposition temperature (IDT) was 100–200 °C, which is due to the loss of moisture or volatile compounds. The second stage was observed in the temperature range of 300 to 500 °C due to the elimination of side chains. Finally, third-stage decomposition was observed at 600 °C due to the breakdown of the crosslinked structure. In comparison, the rate of decomposition was lower in the case of IPNCB than CMC or CB, which indicates the more condensed and stable crosslinked polymeric network in IPNCB. This may be due to the incorporation of biochar into the polymeric network, which provides a protective barrier to both mass and energy transport in the hydrogel composite interpenetrating network.

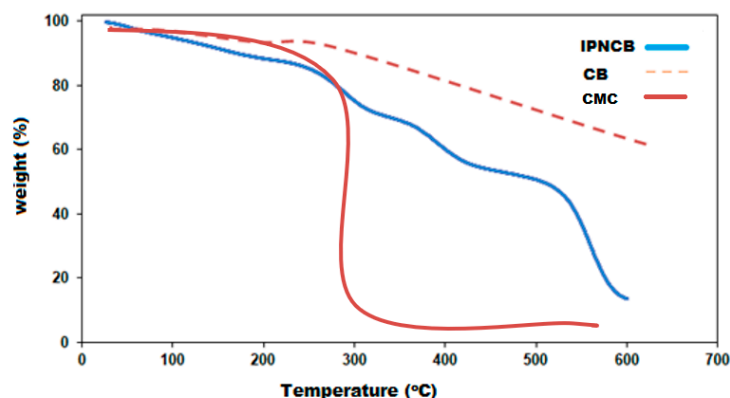


Figure 6. TGA of Carboxy Methyl Cellulose (CMC), Biochar (CB), and Interpenetrating Network Biochar composite (IPNCB).

An increase in hydrothermal severity leads to the generation of hydrochar with higher condensed carbon through the removal of H and O in a coalification-like process. The components of raw biomass go through various degradation processes. The major components

of waste biomass were highlighted for a better understanding of the underlying reactions and the interactions of the components in real biomass conversion during the degradation process [38,39].

### 3.5. Equilibrium Water Absorbency and Swelling Behavior of IPNCB Composite in Different Media

The incorporation of BC into polymer matrix affects EW. The highest equilibrium water swelling, EW value was found to be at the weight ratio of 2% BC. It is clear that in Table 5, maximum equilibrium swelling is about 1900 g/g with microwave synthesis. This may be due to the presence of hydrophilic groups in the matrix structure and the porous property of biochar with high surface area, which enhances and increases water absorbance capacity, and retention of water in the 3D interpenetrating network.

**Table 5.** Effect of CB weight ratio on water absorption capacity.

CB (%)	Equilibrium Swelling (EW)
0	1200
1	1700
2	1900

On the contrary, when the concentration of BC increases, the water absorbance capacity decreases, which may be due to the superiority of the hydrophobic properties over the hydrophilicity of the IPNCB composite with an increase in biochar [40].

The water absorbance of IPNBC composite in s-water 0.9 wt% NaCl solution, as can be seen in Figure 7, shows that the decrease in swelling behavior is relative to the values in d-water. This action is attributed to a charge screening effect of ionic hydrogels [41], producing an imperfect anion–anion repulsion, led to a reduced ionic pressure between the SAP hydrogels and the water molecules, thereby decreasing water absorption capacity. D-water displays good results, as it has lower ionic concentration, which aids in better water intake by osmotic pressure.

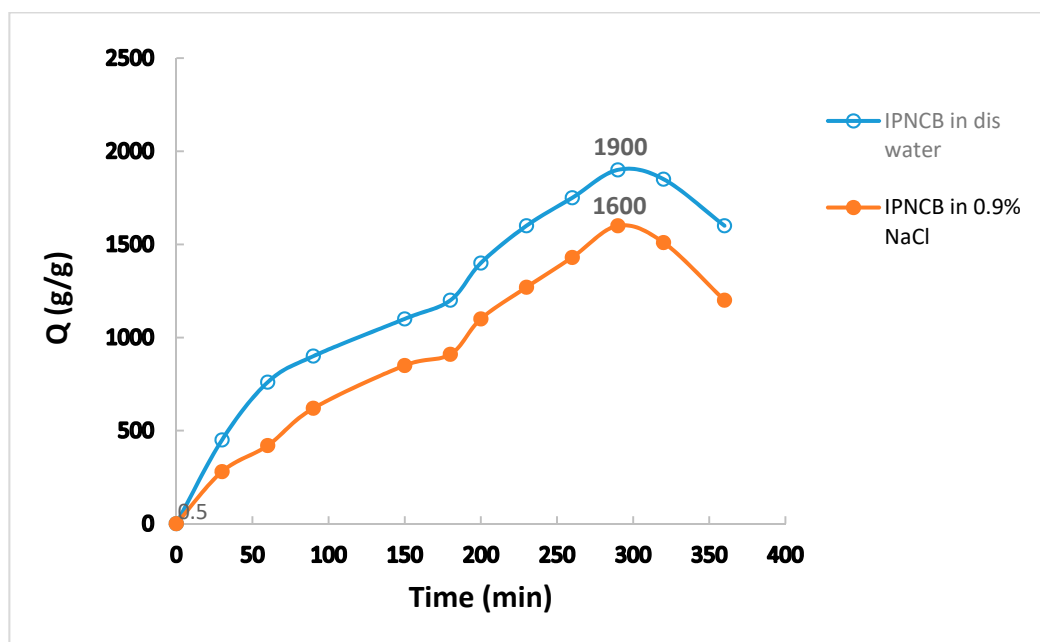


**Figure 7.** Swelling behavior of the IPNCB composite in different media.

Figure 8 shows the equilibrium swelling (EW) of IPNBC composite at different pH values. The IPNBC composite displayed a low EW in acidic media and maximum value in neutral medium. This phenomenon refers to the increase in pH value; carboxyl groups

in the CMC are converted to carboxylate ions, which leads to repulsion and forms space between chains, allowing water particles to enter the IPNCB composite and enhancing water absorption [42]. However, as pH increases above pH 7, absorption capacity is reduced. This is possibly due to the existence of Na<sup>+</sup> cations in basic solutions, which avoid anion–anion repulsion and decrease space between chains, thereby decreasing water absorption capacity [42,43]. Table 6 summarizes the values of EW in different media.

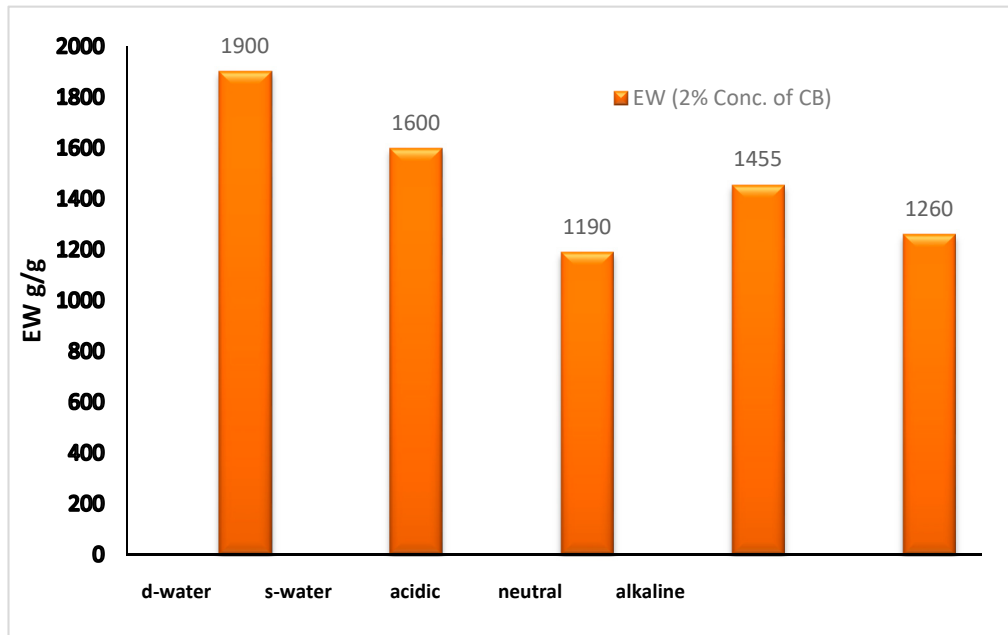


Figure 8. Swelling behavior of the IPNCB composite in different media.

Table 6. Swelling behavior of CMC-g-(TerPolys)/CB in various buffer media.

CB (%)	EW (g/g)
D-water 2	1900
S-water 2	1600
Acidic 2	1190
Neutral 2	1455
Alkaline 2	1260

### 3.6. Physical Properties of the Soil with IPNCB Composite

#### 3.6.1. Water Holding Capacity (WHC)

The WHC% and WR% of soil with various amounts of the IPNCB composite (1% and 2%) are represented in Figures 9 and 10, respectively. The WHC% of soil without composite (0%) was 26%, whereas the WHC% of the treated soil was 41.8% and 57.6% for IPNCB of 1% and 2% (Figure 9). It can be clearly seen that CMC-g-(TerPolys)/BC had an outstanding result on the WHC% of soil, which enhanced with increasing concentration ratio of the IPNCB composite. The higher swelling absorbance (EW) due to existing hydrophilic function groups in polymer composite CMC-g-(AA-Am-AMPS) and BC was proved by the FTIR spectrum [44]. The incorporation of BC in the IPNCB composite enhances water holding due to its highly porous structure, which was confirmed by SEM morphology [45]. The WHC% of soil was 57.6% and 41.8% for CMC-g-(TerPolys)/BC of 1% and 2%. The soil can hold and store a significant amount of water when mixed with a larger ratio of 2% IPNCB composite concentration. As a result, soil wetness is improved, and water consumption is decreased.

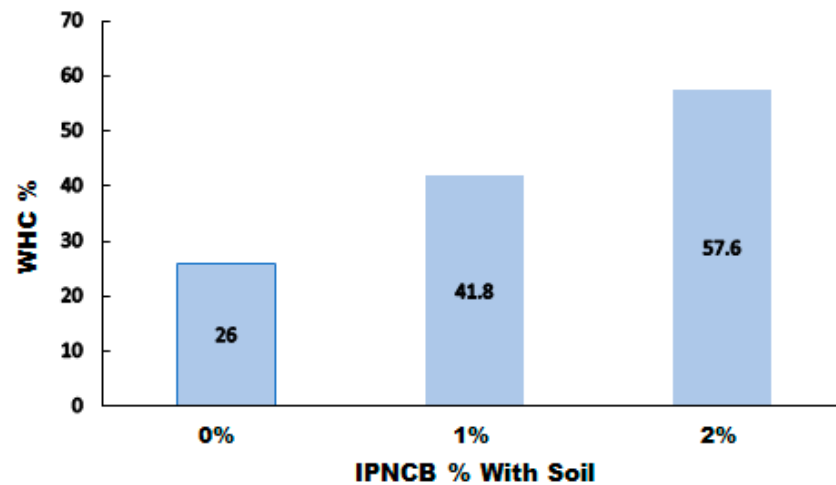


Figure 9. Effect of BC ratio (%) on water holding capacity (WHC).

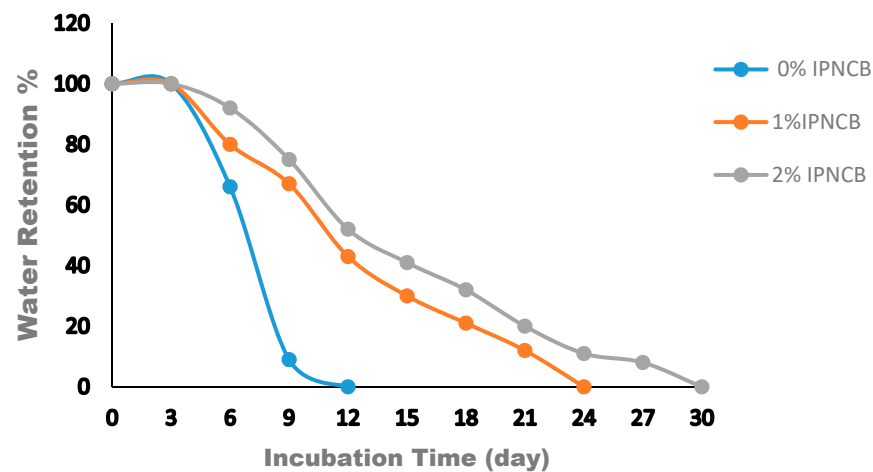


Figure 10. Effect of BC ratio (%) on water retention (WR).

### 3.6.2. Water Retention (WR)

As seen in Figure 10, the water retention of the soil without the IPNCB composite decreases, with all the irrigated water lost over 12 days, while the WR% of the soil mixed with (1% and 2%) of the IPNCB composite was depleted after 24 and 30 days. Therefore, the water retention rate of the soil was increased by adding 2% of the IPNCB composite. This action may be due to the IPNCB composite having many hydrophilic groups and the highly porous structure of BC, which enhances the soil's physical properties and increases water absorption. The prepared IPNCB composite (2%) enhances the WR% of the soil to 9.1% after 30 days. Soil mixed with the prepared IPNCB composite can accordingly improve plant growth and reduce water consumption through irrigation of arid lands. The IPNCB composite is therefore a candidate in agriculture applications.

### 3.7. Degradation Rate of IPNCB in Sandy Soil

Figure 11 shows that the degradation rate of the IPNCB composite in soil after 30 days was calculated to be 23%. Soil is a complex system, including bacteria and enzymes. When the IPNCB composite was buried in the soil, swelling commenced after irrigation of soil, which allowed the interaction of the IPNCB composite with soil containing bacteria and enzymes [46]. IPNCB then started to decompose into small pieces through the hydrolysis of ether bonds (-O-).

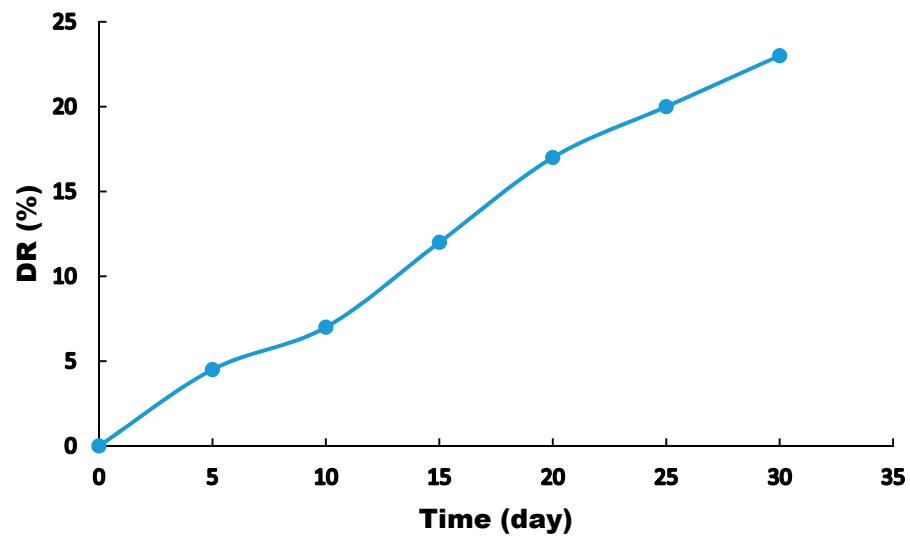


Figure 11. Degradation rate of IPNCB in the soil.

The degradation of TerPolys (AA-co-Am-co-AMPS) and bonds in CMC structure [47] causes a decrease of crosslink density of the IPNCB composite, enabling breakdown of the composite with bacteria and enzymes in the soil. The degradation rate in the present work is in agreement with other studies that found comparable values for similar evaluation times [48], indicating that the IPNCB superabsorbent composite is degradable and could be applied in arid land and various agricultural applications.

### 3.8. Effect of IPNCB Composite on Plant Growth

Further confirming the efficiency of the prepared IPNCB composite on plant growth, as shown in Figure 12, the wheat seedling height and strength of leaves were increased, and leaves were greener in the case of 2% IPNCB than for 1% and 0% IPNCB. It was evident that the addition of IPNCB composite to the soil helped plant growth more than without it. Germination rate was  $90.12 \pm 2.44\%$  in 2% IPNCB as compared to 1% IPNCB ( $88.34 \pm 2.44\%$ ) and 0% IPNCB ( $70.33 \pm 2.44\%$ ). The plant height and root length were increased by addition of IPNCB composite, and all data are summarized in Table 7. This may be attributed to biochar (BC) incorporated into the IPN matrix, which provides nutrients for plants and assists wheat growth.

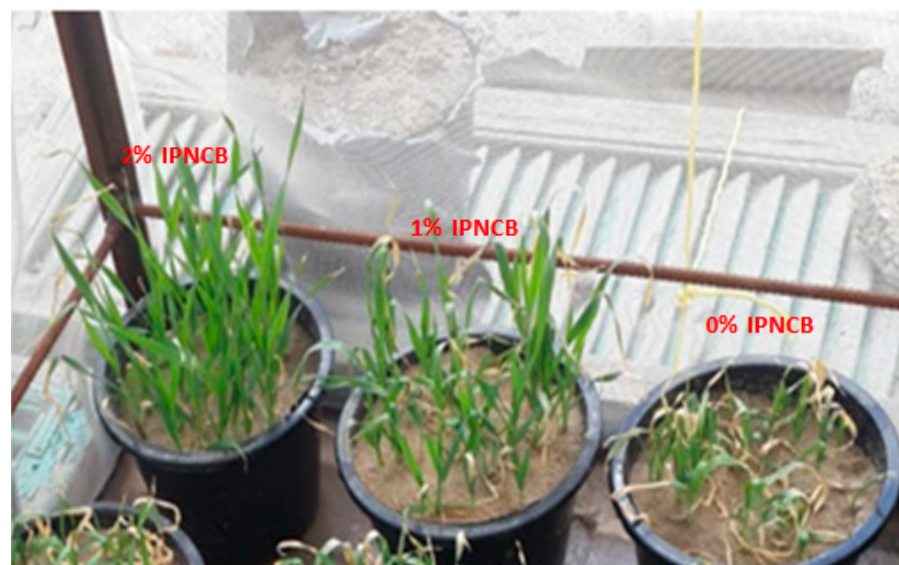


Figure 12. Effect of the IPNCB composite on wheat plant growth.

**Table 7.** Effect of IPNCB Composite on Wheat Plant Growth.

Sample	Hight of Plant (cm)	Length of Roots (cm)	Germination Rate (%)
2% IPNCB	14.3	7.1	90.12 ± 2.44
1% IPNCB	11.5	6.7	88.43 ± 2.44
0% IPNCB	7.3	5.1	70.33 ± 2.44

#### 4. Conclusions

An innovative superabsorbent composite based on biochar grafted on CMC-terpolymers was fabricated (IPNCB) through conventional and microwave methods. The microwave route improved the time of the polymerization reaction and shows high swelling behavior when compared with the conventional technique with optimized monomer, crosslinker, and initiator concentration. The addition of the 2% CB to the polymer matrix results in an improvement in swelling behavior in different media. TGA showed better thermal stability of the IPNCB composite as compared to the blank CMC. The porous structure of the IPNCB shown by SEM proves the incorporation of biochar and CB into the polymer network. In addition, the mixing of the INPCB composite into the studied soil can improve the WHC% and WR% rate of the soil and wheat plant growth. IPNCB shows good degradation rate in the soil, which helps to decrease environmental contamination. The prepared IPNCB composite therefore shows promise in sustainable agriculture irrigation.

**Author Contributions:** Conceptualization, S.M.e.-k., E.G.Z., T.M.I., N.I.T., H.A.S., A.A.G., and S.M.E.; methodology, S.M.E., E.G.Z., T.M.I., N.I.T., and S.M.E.; software, S.M.E., E.G.Z., T.M.I., and S.M.E.; validation, S.M.E., E.G.Z., T.M.I., N.I.T., H.A.S., A.A.G., A.E., and S.M.E.; formal analysis, S.M.E., E.G.Z., T.M.I., and N.I.T.; investigation, S.M.E., E.G.Z., T.M.I., N.I.T., H.A.S., A.A.G., and S.M.E.; resources, S.M.e.-k., E.G.Z., T.M.I., N.I.T., H.A.S., A.A.G., A.E. and S.M.E.; data curation, S.M.e.-k., E.G.Z., T.M.I., N.I.T., H.A.S., A.A.G., and S.M.E.; writing—original draft preparation, S.M.e.-k., E.G.Z., T.M.I., and N.I.T.; writing—review and editing, S.M.e.-k., E.G.Z., T.M.I., N.I.T., H.A.S., A.A.G., A.E. and S.M.E.; visualization, S.M.e.-k., E.G.Z., T.M.I., N.I.T., H.A.S., A.A.G., and S.M.E.; supervision, H.A.S., A.A.G., A.E. and S.M.E.; funding acquisition, H.A.S. and A.A.G. and A.E. All authors have read and agreed to the published version of the manuscript.

**Funding:** This research received no external funding.

**Informed Consent Statement:** Not applicable.

**Acknowledgments:** We thank the researchers at Taif University, Taif, Saudi Arabia (supporting project number: TURSP-2020/07).

**Conflicts of Interest:** The authors declare no conflict of interest.

#### References

- Han, B.; Benner, S.G.; Flores, A.N. Evaluating impacts of climate change on future water scarcity in an intensively managed semi-arid region using a coupled model of biophysical processes and water rights. *Hydrol. Earth Syst. Sci. Discuss.* **2018**, *2017*, 1–53.
- Rashidzadeh, A.; Olad, A. Slow-released NPK fertilizer encapsulated by NaAlg-g-poly (AA-co-AAm)/MMT superabsorbent nanocomposite. *Carbohydr. Polym.* **2014**, *114*, 269–278. [[CrossRef](#)] [[PubMed](#)]
- Abdel-Raouf, M.E.; El-Saeed, S.M.; Zaki, E.G.; Al-Sabagh, A.M. Green chemistry approach for preparation of hydrogels for agriculture applications through modification of natural polymers and investigating their swelling properties. *Egypt. J. Pet.* **2018**, *27*, 1345–1355. [[CrossRef](#)]
- Hasija, V.; Sharma, K.; Kumar, V.; Sharma, S.; Sharma, V. Green synthesis of agar/Gum Arabic based superabsorbent as an alternative for irrigation in agriculture. *Vacuum* **2018**, *157*, 458–464. [[CrossRef](#)]
- El-Kafrawy, A.F.; El-Saeed, S.M.; Farag, R.K.; El-Saeed, H.A.-A.; Abdel-Raouf, M.E.-S. Adsorbents based on natural polymers for removal of some heavy metals from aqueous solution. *Egypt. J. Pet.* **2017**, *26*, 23–32. [[CrossRef](#)]
- Abdul-Raheim, A.-R.M.; El-Saeed Shima, M.; Farag, R.K.; Abdel-Raouf Manar, E.; Reem, K.F.; Abdel-Raouf Manar, E. Low cost biosorbents based on modified starch iron oxide nanocomposites for selective removal of some heavy metals from aqueous solutions. *Adv. Mater. Lett.* **2016**, *7*, 402–409. [[CrossRef](#)]

7. Farag, R.K.; El-Saeed, S.M.; Abdel-Raouf, M.E. Synthesis and investigation of hydrogel nanoparticles based on natural polymer for removal of lead and copper(II) ions. *Desalination Water Treat.* **2015**, *57*, 16150–16160. [[CrossRef](#)]
8. Peppas, N.A.; Van Blarcom, D.S. Hydrogel-based biosensors and sensing devices for drug delivery. *J. Control. Release* **2016**, *240*, 142–150. [[CrossRef](#)]
9. Chen, Y.; Tan, Z.; Wang, W.; Peng, Y.-Y.; Narain, R. Injectable, Self-Healing, and Multi-Responsive Hydrogels via Dynamic Covalent Bond Formation between Benzoxaborole and Hydroxyl Groups. *Biomacromolecules* **2019**, *20*, 1028–1035. [[CrossRef](#)]
10. Yuan, T.; Zhang, L.; Li, K.; Fan, H.; Fan, Y.; Liang, J.; Zhang, X. Collagen hydrogel as an immunomodulatory scaffold in cartilage tissue engineering. *J. Biomed. Mater. Res. Part B Appl. Biomater.* **2013**, *102*, 337–344. [[CrossRef](#)]
11. Ahmad, M.; Zhang, B.; Wang, J.; Xu, J.; Manzoor, K.; Ahmad, S.; Ikram, S. New method for hydrogel synthesis from diphenylcarbazide chitosan for selective copper removal. *Int. J. Biol. Macromol.* **2019**, *136*, 189–198. [[CrossRef](#)]
12. Du, H.; Shi, S.; Liu, W.; Teng, H.; Piao, M. Processing and modification of hydrogel and its application in emerging contaminant adsorption and in catalyst immobilization: A rev1. *Environ. Sci. Pollut. Res.* **2020**, *27*, 12967–12994. [[CrossRef](#)]
13. Akl, Z.F.; El-Saeed, S.M.; Atta, A.M. In-situ synthesis of magnetite acrylamide amino-amidoxime nanocomposite adsorbent for highly efficient sorption of U(VI) ions. *J. Ind. Eng. Chem.* **2016**, *34*, 105–116. [[CrossRef](#)]
14. El-Hoshoudy, A.; Zaki, E.; Elsaheed, S. Experimental and Monte Carlo simulation of palmitate-guar gum derivative as a novel flooding agent in the underground reservoir. *J. Mol. Liq.* **2020**, *302*, 112502. [[CrossRef](#)]
15. El-hoshoudy, A.N.; Zaki, E.G.; Elsaheed, S.M. Biopolymers composites as oil improving candidates-article review. *Pet. Coal* **2019**, *61*, 1365–1377.
16. Kluczka, J.; Gnus, M.; Kazek-Kęsik, A.; Dudek, G. Zirconium-chitosan hydrogel beads for removal of boron from aqueous solutions. *Polymer* **2018**, *150*, 109–118. [[CrossRef](#)]
17. Demitri, C.; Scalera, F.; Madaghiele, M.; Sannino, A.; Maffezzoli, A. Potential of Cellulose-Based Superabsorbent Hydrogels as Water Reservoir in Agriculture. *Int. J. Polym. Sci.* **2013**, *2013*, 435073. [[CrossRef](#)]
18. Yoon, S.-D. Cross-Linked Potato Starch-Based Blend Films Using Ascorbic Acid as a Plasticizer. *J. Agric. Food Chem.* **2013**, *62*, 1755–1764. [[CrossRef](#)]
19. Chandrika, K.P.; Singh, A.; Rathore, A.; Kumar, A.; Poorna, C.K. Novel cross linked guar gum-g-poly(acrylate) porous superabsorbent hydrogels: Characterization and swelling behaviour in different environments. *Carbohydr. Polym.* **2016**, *149*, 175–185. [[CrossRef](#)] [[PubMed](#)]
20. Nnadi, F.; Brave, C. Environmentally friendly superabsorbent polymers for water conservation in agricultural lands. *J. Soil Sci. Environ. Manag.* **2011**, *2*, 206–211.
21. Refat, M.S.; Ibrahim, H.K.; Sowellim, S.Z.A.; Soliman, M.H.; Saeed, E.M. Spectroscopic and Thermal Studies of Mn(II), Fe(III), Cr(III) and Zn(II) Complexes Derived from the Ligand Resulted by the Reaction between 4-Acetyl Pyridine and Thiosemicarbazide. *J. Inorgan. Organomet. Polym. Mater.* **2009**, *19*, 521–531. [[CrossRef](#)]
22. Samak, D.H.; El-Sayed, Y.S.; Shaheen, H.M.; El-Far, A.H.; Abd El-Hack, M.E.; Noreldin, A.E.; El-Naggar, K.; Abdelnour, S.A.; Saied, E.M.; El-Seedi, H.R.; et al. Developmental Toxicity of Carbon Nanoparticles during Embryogenesis in Chicken. *Environ. Sci. Pollut. Res.* **2020**, *27*, 19058–19072. [[CrossRef](#)]
23. Saied, E.M.; Banhart, S.; Bürkle, S.E.; Heuer, D.; Arenz, C. A Series of Ceramide Analogs Modified at the 1-Position with Potent Activity against the Intracellular Growth of Chlamydia Trachomatis. *Future Med. Chem.* **2015**, *7*, 1971–1980. [[CrossRef](#)]
24. Xiao, R.; Awasthi, M.K.; Li, R.; Park, J.; Pensky, S.M.; Wang, Q.; Wang, J.J.; Zhang, Z. Recent developments in biochar utilization as an additive in organic solid waste composting: A review. *Bioresour. Technol.* **2017**, *246*, 203–213. [[CrossRef](#)]
25. Tang, J.; Mu, B.; Zong, L.; Wang, A. From waste hot-pot oil as carbon precursor to development of recyclable attapulgite/carbon composites for wastewater treatment. *J. Environ. Sci.* **2019**, *75*, 346–358. [[CrossRef](#)]
26. Sial, T.A.; Lan, Z.; Khan, M.N.; Zhao, Y.; Kumbhar, F.; Liu, J.; Zhang, A.; Hill, R.L.; Lahori, A.H.; Memon, M. Evaluation of orange peel waste and its biochar on greenhouse gas emissions and soil biochemical properties within a loess soil. *Waste Manag.* **2019**, *87*, 125–134. [[CrossRef](#)] [[PubMed](#)]
27. Kim, H.S.; Yun, S.G.; Kweon, U.G.; Park, S.B.; Chung, E.S.; Kang, W.S. Seasonal difference in aerobic storage, ruminal degradation and chemical composition of wet brewers' grain. *RDA J. Agric. Sci. (Korea Repub.)* **1996**, *38*, 609.
28. Zhang, M.; Cheng, Z.; Zhao, T.; Liu, M.; Hu, M.; Li, J. Synthesis, Characterization, and Swelling Behaviors of Salt-Sensitive Maize Bran–Poly(acrylic acid) Superabsorbent Hydrogel. *J. Agric. Food Chem.* **2014**, *62*, 8867–8874. [[CrossRef](#)] [[PubMed](#)]
29. Kuang, J.; Yuk, K.Y.; Huh, K.M. Polysaccharide-based superporous hydrogels with fast swelling and superabsorbent properties. *Carbohydr. Polym.* **2011**, *83*, 284–290. [[CrossRef](#)]
30. Sharma, K.; Kaith, B.; Kumar, V.; Kalia, S.; Kumar, V.; Swart, H. Water retention and dye adsorption behavior of Gg-cl-poly(acrylic acid-aniline) based conductive hydrogels. *Geoderma* **2014**, *232*, 45–55. [[CrossRef](#)]
31. Casaburi, A.; Rojo, Ú.M.; Cerrutti, P.; Vázquez, A.; Foresti, M.L. Carboxymethyl cellulose with tailored degree of substitution obtained from bacterial cellulose. *Food Hydrocoll.* **2018**, *75*, 147–156. [[CrossRef](#)]
32. Peng, Z.; Chen, F. Synthesis and Properties of Lignin-Based Polyurethane Hydrogels. *Int. J. Polym. Mater.* **2011**, *60*, 674–683. [[CrossRef](#)]
33. Sen, G.; Mishra, S.; Jha, U.; Pal, S. Microwave initiated synthesis of polyacrylamide grafted guar gum (GG-g-PAM)—Characterizations and application as matrix for controlled release of 5-amino salicylic acid. *Int. J. Biol. Macromol.* **2010**, *47*, 164–170. [[CrossRef](#)] [[PubMed](#)]

34. Anbarasan, R.; Jayaseharan, J.; Sudha, M.; Nirmala, P.V.; Gopalan, A. Peroxydisulphate initiated graft copolymerization of o-toluidine onto synthetic fibres—A kinetic approach. *Macromol. Chem. Phys.* **2000**, *201*, 1869–1876. [[CrossRef](#)]
35. Flory, P.J. *Principles of Polymer Chemistry*; Cornell University Press: Ithaca, NY, USA, 1953.
36. Wang, W.B.; Wang, A.Q. Preparation, Swelling and Water-Retention Properties of Crosslinked Superabsorbent Hydrogels Based on Guar Gum. *Adv. Mater. Res.* **2010**, *96*, 177–182. [[CrossRef](#)]
37. Takaya, C.; Fletcher, L.; Singh, S.; Anyikude, K.; Ross, A. Phosphate and ammonium sorption capacity of biochar and hydrochar from different wastes. *Chemosphere* **2016**, *145*, 518–527. [[CrossRef](#)]
38. Wang, T.; Liu, X.; Wang, D.; Gong, Z.; Si, B.; Zhai, Y. Persulfate assisted hydrothermal processing of spirulina for enhanced deoxidation carbonization. *Bioresour. Technol.* **2021**, *322*, 124543. [[CrossRef](#)]
39. Wang, T.; Zhai, Y.; Zhu, Y.; Li, C.; Zeng, G. A review of the hydrothermal carbonization of biomass waste for hydrochar formation: Process conditions, fundamentals, and physicochemical properties. *Renew. Sustain. Energy Rev.* **2018**, *90*, 223–247. [[CrossRef](#)]
40. Fang, Q.; Chen, B.; Lin, Y.; Guan, Y. Aromatic and Hydrophobic Surfaces of Wood-derived Biochar Enhance Perchlorate Adsorption via Hydrogen Bonding to Oxygen-containing Organic Groups. *Environ. Sci. Technol.* **2014**, *48*, 279–288. [[CrossRef](#)]
41. Zhao, Y.; Su, H.; Fang, L.; Tan, T. Superabsorbent hydrogels from poly (aspartic acid) with salt-, temperature- and pH-responsiveness properties. *Polymer (Guildf.)* **2005**, *46*, 5368–5376. [[CrossRef](#)]
42. Wang, W.; Wang, Q.; Wang, A. pH-responsive carboxymethylcellulose-g-poly (sodium acrylate)/polyvinylpyrrolidone semi-IPN hydrogels with enhanced responsive and swelling properties. *Macromol. Res.* **2011**, *19*, 57–65. [[CrossRef](#)]
43. Priyadarshi, R.; Kumar, B.; Rhim, J.-W. Green and facile synthesis of carboxymethylcellulose/ZnO nanocomposite hydrogels crosslinked with Zn<sup>2+</sup> ions. *Int. J. Biol. Macromol.* **2020**, *162*, 229–235. [[CrossRef](#)]
44. Sanyang, M.; Ghani, W.A.W.A.K.; Idris, A.; Bin Ahmad, M. Hydrogel biochar composite for arsenic removal from wastewater. *Desalin. Water Treat.* **2016**, *57*, 3674–3688. [[CrossRef](#)]
45. Wang, Y.; Liu, M.; Ni, B.; Xie, L. κ-Carrageenan–sodium alginate beads and superabsorbent coated nitrogen fertilizer with slow-release, water-retention, and anticompaction properties. *Ind. Eng. Chem. Res.* **2012**, *51*, 1413–1422. [[CrossRef](#)]
46. Lü, S.; Feng, C.; Gao, C.; Wang, X.; Xu, X.; Bai, X.; Gao, N.; Liu, M. Multifunctional environmental smart fertilizer based on l-aspartic acid for sustained nutrient release. *J. Agric. Food Chem.* **2016**, *64*, 4965–4974. [[CrossRef](#)] [[PubMed](#)]
47. Jin, S.; Wang, Y.; He, J.; Yang, Y.; Yu, X.; Yue, G. Preparation and properties of a degradable interpenetrating polymer networks based on starch with water retention, amelioration of soil, and slow release of nitrogen and phosphorus fertilizer. *J. Appl. Polym. Sci.* **2012**, *128*, 407–415. [[CrossRef](#)]
48. Wang, X.; Lü, S.; Gao, C.; Xu, X.; Wei, Y.; Bai, X.; Feng, C.; Gao, N.; Liu, M.; Wu, L. Biomass-based multifunctional fertilizer system featuring controlled-release nutrient, water-retention and amelioration of soil. *RSC Adv.* **2014**, *4*, 18382–18390. [[CrossRef](#)]